Predicting plant diversity in revegetated grasslands with Sentinel-2: comparing performance of spatio-temporal features with input time series

Pinja Lindgrén[1], Matthieu Molinier[1], Alexander Kießling[2], Astrid Tischler[2]

[1] VTT Technical Research Centre of Finland Ltd, PL1000 - TE1, 02044 VTT, Finland
(pinja.lindgren, matthieu.molinier)@vtt.fi
[2] Bonatica, Hall in Tirol, Austria(akiessling00, astrid.tischler25)@gmail.com

Keywords: Sentinel-2, Time series descriptors, Biodiversity, Species Richness, Alpine grasslands

Abstract

Mining companies are continuously looking for cost efficient methods to monitor the success of their rehabilitation efforts. Although open access satellite imagery is available at regular temporal intervals, its usefulness for grassland biodiversity monitoring has been questioned due to its coarse spatial resolution with respect to the species size. To compensate for the low spatial resolution, previous studies have successfully explored the benefits of using a multitemporal set of Sentinel-2 (S2) images. However, unless the temporal patterns are studied as a whole, some of the phenological information such as growth rates are lost, and delayed snow cover may spread events like growth onset over multiple dates between plots. This study aims to explore the added value of temporal fitting of Sentinel-2 time series (ts) over existing baseline models applied using the full time series as such. Our set of temporal features included functional components, harmonic decomposition, frequency decomposition, and phenological metrics. Out of the compared models, the Random Forest regression model using a set of fitted temporal features achieved the highest holdout prediction accuracy (R2 = 0.36, RMSE = 3.87, relative RMSE = 0.20) and cross-validation accuracy similar to the baseline models. However, all the compared regression models underestimated extreme plant diversity to some extent. Future studies should account for varying vegetation cover and terrain features by incorporating auxiliary data.

1. Introduction

Environment monitoring legislation expects mining companies to perform field evaluations to demonstrate their rehabilitation efforts and success (McKenna et al., 2020). However, traditional evaluation methods such as in-field transects and quadrat monitoring alone often cover only a small portion of the mine site and are restricted by accessibility on foot. Permanent plots are rarely possible in or around mine sites, or in surrounding land uses, e.g., pasture with grazing cattle. Remotely Sensed low-cost satellite imagery has the potential to expand both spatial and temporal coverages of field surveys. However, the low spatial resolution of satellites in relation to grassland species dimensions is not suited for direct within pixel species identification, even at the highest available spatial resolutions (Yang et al., 2025).

Previous studies have suggested compensating for the limited spatial resolution with temporal variation observed in Sentinel-2 image time series when modeling grassland diversity patterns (Fauvel et al., 2020, Muro et al., 2022). However, most of these existing multitemporal grassland studies still focus on finding the key image acquisition dates from a full time series instead of observing the temporal patterns over the growing season. Providing the full time series as input to the modeling algorithm also requires a large reference dataset which is difficult to acquire for a local biodiversity study.

In order to evaluate the predictive ability of Sentinel-2 imagery more completely, this study extracts various temporal features from a dense multi-year time series (Molinier et al., 2021). The aim is to capture the overall temporal behavior of the grassland pixels with a reduced number of variables, compared to inserting all available time series observations into a model. The extracted features cover metrics from phenological key dates to functional coefficients and frequency analysis. Several years have been assessed together to repair cloud-induced gaps and other unexpected weather events. The performance of the extracted features is compared to the full set of temporal observations used in previous multitemporal studies.

2. Study area and data

The vegetation study area is located around an active open pit magnesite mine site in Hochfilzen, Austria (Figure 1). The surroundings of the site represent mountainous alpine grasslands which have been undergoing revegetation work in several periods since 1971. For the studied subareas, the revegetation began 10 to 40 years ago. Some of these areas are already in succession.

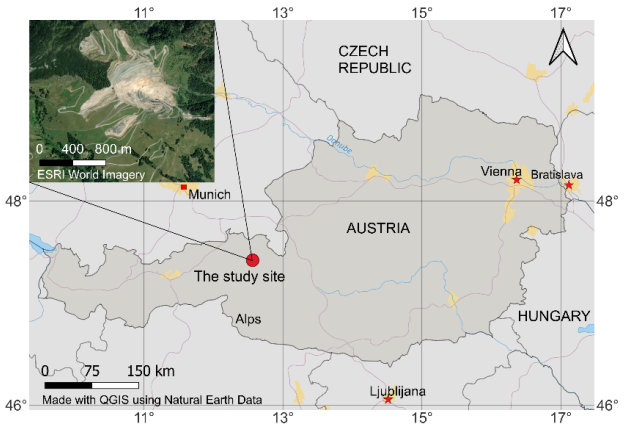

Figure 1. Location and overview of the study site.

This contribution has been peer-reviewed. The double-blind peer-review was conducted on the basis of the full paper.
https://doi.org/10.5194/isprs-annals-XI-3-2026-749-2026 | © Author(s) 2026. CC BY 4.0 License.

The vegetation varies from recultivated alpine meadow and pasture, to natural succession where shrubs and young deciduous trees, mostly shorter than 2m, can be found. Further from the open pit, natural pasture and grazed ski slopes are also present.

2.1 In situ data

In situ data was collected in July 2024 from 77 measurement quadrats (1m x 1m) aligned with Sentinel-2 (S2) pixel centers, as in Figure 2. For each quadrat, the plant diversity was estimated with the number of species, i.e., Species Richness (SR). The observed Species Richness varied from 3 to 31 species per quadrat (Figure 3).

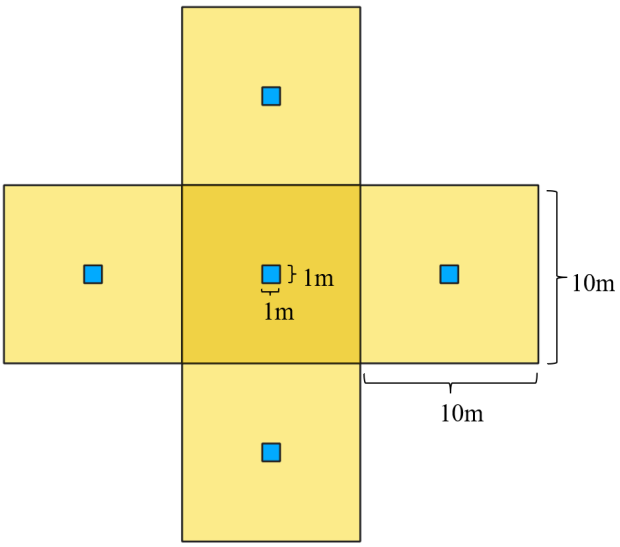

Figure 2. 1m x 1m quadrat placement in relation to the 10m Sentinel-2 pixel. The surrounding pixels were measured only for the quadrat clusters.

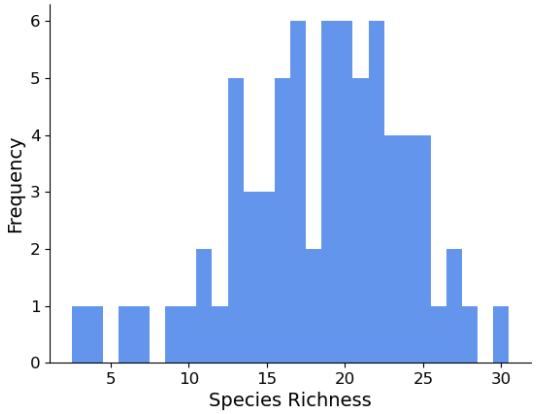

Figure 3. Distribution of the 77 Species Richness measurements in Hochfilzen, 2024.

The placement of the quadrats was stratified to ensure that each grassland type at the site was represented in relation to its spatial coverage (Figure 4). Most of the quadrat locations followed random sampling with a minimum distance of 60m. For each of the five largest grassland patches, one quadrat cluster of neighboring pixels (Figure 2) was included, inspired by (Fauvel et al., 2020).

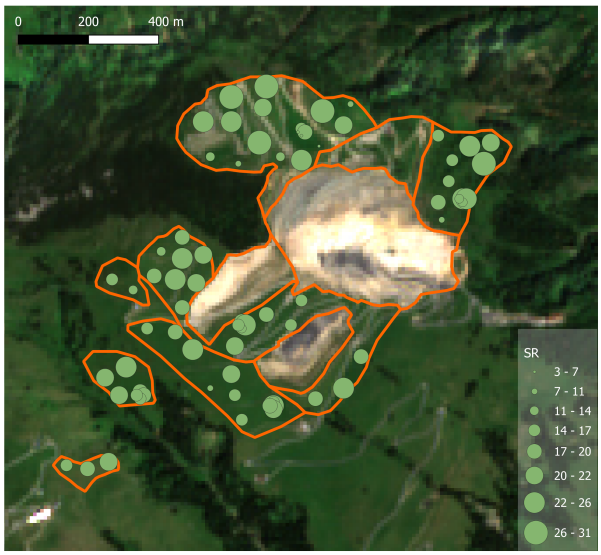

Figure 4. Spatial distribution of the Species Richness quadrats.

2.2 Remote sensing data and pre-processing

A dense cloud masked Sentinel-2 time series from 2020 to 2024 was created from all available Level-2A imagery, processed with the Sen2Cor algorithm.

3. Methods

3.1 Time series feature extraction

Five vegetation indices (VI) were considered for time series feature extraction. The vegetation index time series for Normalized Difference Vegetation Index (NDVI), Enhanced 2-band Vegetation Index (EVI2), Normalized Difference Red-Edge (NDRE), Chlorophyll Index Red-Edge (CIRE), and NIR/Green-ratio (NIRGreen) were computed from the Sentinel-2 imagery to highlight temporal changes related to productivity and pigment changes.

For each VI, four sets of time series features were extracted:

- Phenological metrics: VI values around the start, end and peak of growing season, rate of increase and decrease, annual mean, integral and length of season,
- Functional Principal Component Analysis (FPCA) components (Ramsay, 2005): 7 pixel-wise scores each corresponding to one basis function of time,
- Harmonic decomposition: constant term, first and second sine and cosine components, amplitudes and phases of the harmonic components, and RMSE of the fitted curve,
- Lomb-Scargle periodogram (Lomb, 1976, Scargle, 1982): powers and ratios of total power explained by 8 frequency bins, and the power at peak frequency.

The growing season for the phenological metrics was defined as the time period which exceeded the 20% threshold of the seasonal amplitude.

Depending on the feature set, the irregular temporal sampling of S2 imagery was adjusted or gap-filled using either spline fitting,

linear interpolation, or LOESS smoothing algorithm (Cleveland and Devlin, 1988):

- For extracting phenological metrics, succeeding years were collapsed into a single Day-Of-Year (DOY) series (Figure 5), and smoothed to daily resolution with LOESS.
- FPCA was performed on a weekly time series smoothed with cubic splines.
- Irregular multiyear time series were used as such to extract harmonic decomposition with Harmonic Analysis Penalty Operator (HAPO) (Zhou et al., 2022) and dominant frequency analysis with Lomb-Scargle periodogram.

Compared to other harmonic fitting algorithms, HAPO applies an in-built penalty operator designed to restrict the length of the harmonic curve in the presence of gaps. Example of the HAPO fit for one of the quadrats is shown in Figure 6. Similarly, Lomb-Scargle is designed to fit sinusoidal functions on unevenly sampled data. It searches periodical signals from a defined range of frequencies, instead of specific frequencies.

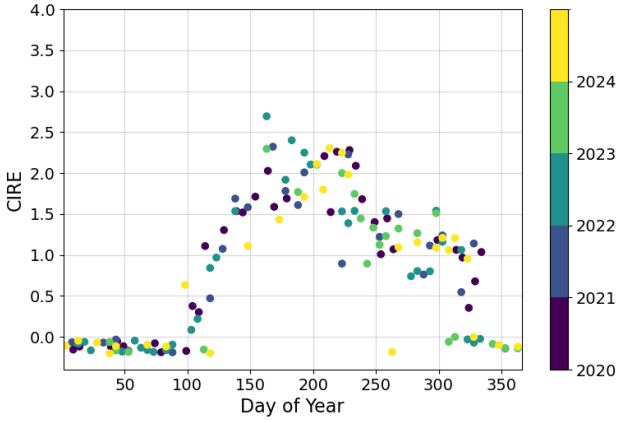

Figure 5. 5-year CIRE time series for one quadrat collapsed into one DOY series.

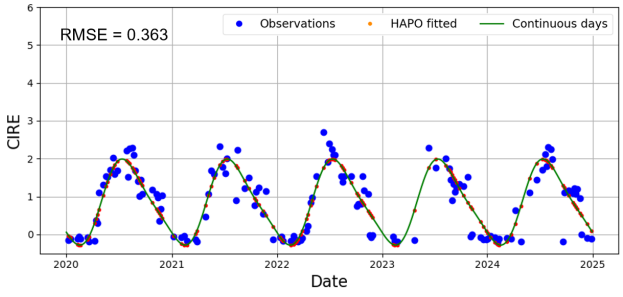

Figure 6. Example of HAPO fit on one of the quadrats.

The performance of the proposed time series feature models was compared to two types of baseline models, which relied on regularly interpolated Sentinel-2 band time series. The first baseline model relied on a 10-band time series interpolated to every 14 days using radial basis function interpolation as in (Muro et al., 2022). We refer to this model as the Muro 10-band ts baseline model. The second baseline model used a re-sampled and gap-filled time series of 2 to 4-bands, with 10 days interval as in (Fauvel et al., 2020). Since Fauvel et al. observed similar predictive performance for 4-band RGB-NIR ts model and 2-band R-NIR ts model, both versions are included here as baselines.

We also added a similarly derived 2-band RE1-NIR ts baseline model, to allow a better comparison with our CIRE temporal features. For each baseline model, a version with and without the feature selection (of maximum of six features) was included, to allow for a fair comparison to our models on a small sample size.

3.2 Modelling

Species Richness was modelled using Random Forest (RF) regression with various combinations of the time series features. First, a nested LeaveOneGroupOut (LOGO) cross-validation was implemented to assess the generalizability of the regression model on new data. Moran's I test indicated presence of spatial autocorrelation only within the quadrat clusters (Figure 2). Therefore each group in LOGO was either a single quadrat or a cluster of five quadrats from the neighboring pixels as in (Fauvel et al., 2020).

Independence of the training and validation data was ensured by providing the same grouping for the inner loop. The inner loop performed a grouped 4-Fold cross-validation for feature selection and hyperparameter tuning. The outer loop predicted plant diversity in the left-out group using the best parameters and the six features selected by SelectFromModel from scikit-learn. Eventually, the predictions for the left-out groups were pooled for accuracy estimation.

After completing the nested LOGO cross-validation, the same GridSearch pipeline was implemented once on all the training and validation data to select one best performing model for wall-to-wall mapping. The performance of this final model was evaluated against 25% holdout test data. Shapley Additive exPlanations (SHAP) (Lundberg and Lee, 2017) importances were added to increase the interpretability of the final model.

4. Results

4.1 Quantitative results

The most consistently high predictions for both holdout and cross-validated data were achieved with temporal features extracted from CIRE vegetation index. For the pooled LOGO cross-validation data (Table 1), the best performing CIRE temporal feature model achieved Coefficient of determination $R^2 = 0.19$, Mean Square Error (MAE) = 3.91, Root Mean Square Error (RMSE) = 5.15, and Relative RMSE (RRMSE) = 29%. Performance of baseline models as published in (Fauvel et al., 2020) and (Muro et al., 2022) was poor on all metrics, likely due to a too large dimensionality of input features leading to overfitting. When restricting the amount of features to 6 to allow a more fair comparison, the performance of baseline models improved noticeably. Our proposed model was still comparable to the best baseline model using input time series of Red Edge1 (RE1) and NIR bands (Fauvel RE1-NIR ts(6))(Table 1), although with a slightly lower R^2.

The holdout set showed the highest performance (R2 = 0.36) for the final CIRE temporal features pipeline (Table 2), clearly outperforming both original baseline models and baseline models restricted to 6 input features. Compared to CIRE, a common challenge for the other considered vegetation indices was the high disagreement between the best performing features selected by the inner 4-Fold cross-validation versus the final model.

Workflow and Predictors	R^2	RMSE	RRMSE
No feature selection			
Fauvel R-NIR ts	0.07	5.50	0.30
Fauvel RE1-NIR ts	0.09	5.44	0.30
Fauvel RGB-NIR ts	0.12	5.37	0.30
Muro 10-band ts	0.05	5.56	0.31
6 best features			
Fauvel R-NIR ts(6)	0.16	5.25	0.29
Fauvel RE1-NIR ts(6)	**0.23**	**5.00**	**0.28**
Fauvel RGB-NIR ts(6)	0.22	5.06	0.28
Muro 10-band ts(6)	0.15	5.27	0.29
CIRE temporal features	0.19	5.15	0.29

Table 1. Accuracy assessment of the nested LeaveOneGroupOut cross-validated SR predictions.

Workflow and Predictors	R^2	RMSE	RRMSE
No feature selection			
Fauvel R-NIR ts	0.21	4.30	0.23
Fauvel RE1-NIR ts	0.10	4.59	0.24
Fauvel RGB-NIR ts	0.11	4.57	0.24
Muro 10-band ts	0.17	4.41	3.65
6 best features			
Fauvel R-NIR ts(6)	0.24	4.22	0.22
Fauvel RE1-NIR ts(6)	0.03	4.78	0.25
Fauvel RGB-NIR ts(6)	0.22	4.26	0.23
Muro 10-band ts(6)	0.10	4.59	0.24
CIRE temporal features	**0.36**	**3.87**	**0.20**

Table 2. Accuracy assessment of the holdout SR predictions.

The most stable model between cross-validated and holdout datasets was the linearly interpolated RGB-NIR model suggested by (Fauvel et al., 2020), restricted to 6 features (Fauvel RGB-NIR ts(6)). However, it was clearly outperformed by the proposed model with CIRE temporal features during holdout evaluation (Table 2). Conversely, the 2-band RE1-NIR model using the same bands as CIRE completely lost its explanatory power on the holdout data. Part of the reason may be suboptimal feature selection when training the final model on all training data. Nevertheless, for the majority of the baseline models, restricting the maximum number of features to six dates during RF regression generally improved the predictive performance (Table 1; Table 2). Therefore, all the figures shown later in the results correspond to the models which incorporated the feature selection.

Overall, the ability to explain variation in grassland Species Richness at Hochfilzen using Sentinel-2 imagery was relatively low for both the temporal features and the full baseline time series. Many of the quadrats with moderate diversity around 18 species received similar predictions and extreme species richness was often eroded closer to the mean. Figure 7 demonstrates this by presenting the pooled LOGO cross-validation predictions (a) for the most consistently performing baseline model with 6 features, Fauvel RGB-NIR ts(6), and (b) for the proposed CIRE temporal features model. Similar pattern as in Figure 7 (a), was observed for the other three baseline models as well.

4.2 Feature importance analysis

Despite varying which input bands were provided, the SHAP feature importance analysis revealed that none of the Red-Edge band dates were selected by the baseline models for the final model training. The baseline models, including the Fauvel RE1-NIR and Muro 10-band models which had access to the 20m bands, preferred NIR and all other 10m resolution bands over the coarser Red-Edge and SWIR bands (Figure 8 (a)). The Red-Edge region was only found important after applying temporal fitting, as suggested by the holdout performance of the proposed CIRE temporal features model (Table 2).

Similarly to the baseline models, which highlighted the importance of the dates around the peak growing season (Figure 8 (a)), many of the selected temporal features were related to the peak growth stage. According to the SHAP feature importance analysis (Figure 8 (b)), the best performing temporal features for CIRE were the 5th FPCA component ($CIRE\_coef5$), the power at peak frequency ($CIRE\_p\_peak$), the share of total power explained by the frequencies centered at 0.5 cycles per year ($CIRE\_above\_annual\_ratio$), the amplitude of season ($CIRE\_aos\_values$), the second harmonic cosine term ($CIRE\_cos2$), and the cumulative CIRE normalized by the length of the growing season ($CIRE\_prod\_values$). Out of these features, especially $CIRE\_p\_peak$ and $CIRE\_aos\_values$ have direct relation to the peak growth.

The placement of the samples on the SHAP value axis in Figure 8 reveals the direction towards which the high (pink) versus the low values (blue) of each feature were driving Species Richness estimates. For example, high NIR reflectance around the peak growing season, which indicates dense green vegetation, was consistently associated with lower richness by the baseline models. The peak growth related CIRE temporal features agreed with this association.

4.3 Final model and wall-to-wall species richness prediction

From the holdout accuracy plots of the final models (Figure 9), we observed that the CIRE temporal features (b) differed from the baseline models (a) in providing slightly higher predictions for the most species rich holdout samples. Although the tendency of RF towards the mean prediction is shown in both subfigures, the final models could find several relative differences in species diversity.

To demonstrate the usage of the final model, we expanded the spatial extent of the model predictions to cover the whole grassland polygons by computing wall-to-wall species richness maps (Figure 10). Only the results for the most consistently performing baseline model (RGB-NIR) and the proposed model are shown for clarity. However, the other baseline models either shared similar characteristics as the RGB-NIR baseline model or showed less separation between the high and the mean richness. As can be seen from wall-to-wall maps, the final models differed mainly in their sensitivity to vegetation cover. Especially in the northernmost parts, CIRE temporal features (Figure 10 (b)) associated areas with low plant cover more closely with high diversity in the wall-to-wall maps than the baseline models (Figure 10 (a)). Instead, the low-diversity regions near the tree line or around the densely vegetated sub-areas matched well across the models.

5. Discussion

Since the reference dataset for Hochfilzen site was smaller than the ones used in the baseline articles by (Fauvel et al., 2020) and (Muro et al., 2022), overly complex models had to be avoided. Therefore, we restricted the RF tree depth to three and the number of selected input features to six. Despite these restrictions, especially the 14-day RBF interpolated 10-band time

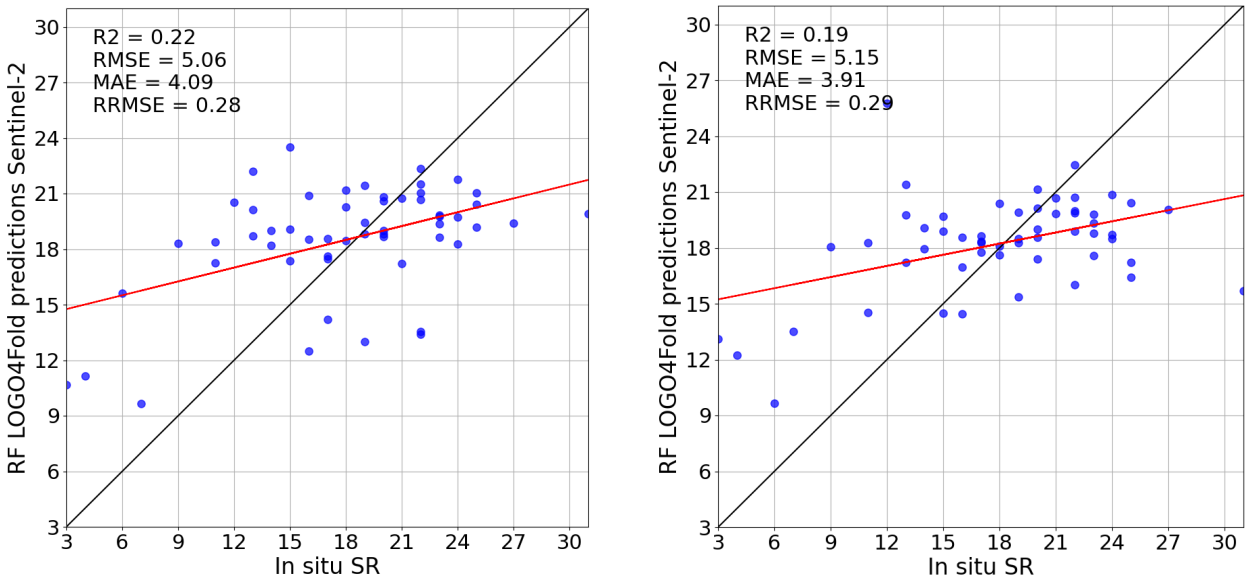

(a) RGB-NIR ts(6) baseline model (Fauvel et al., 2020), with 6 best features (dates)

(b) Proposed CIRE temporal features model

Figure 7. Pooled SR predictions of the nested LOGO cross-validation

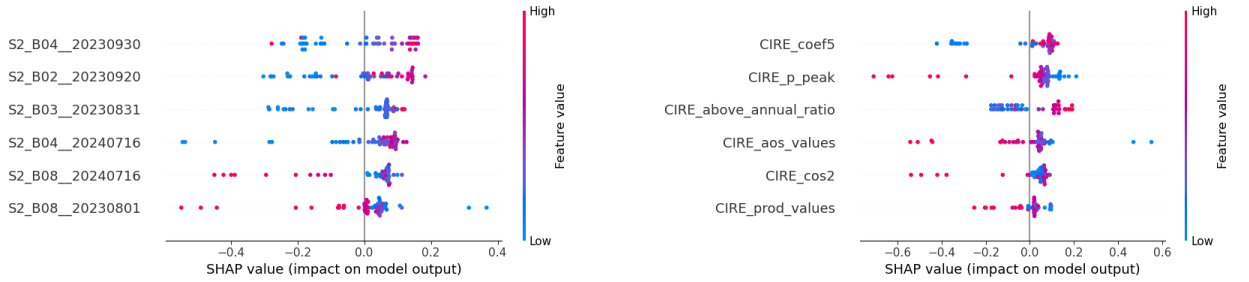

(a) RGB-NIR ts(6) baseline model (Fauvel et al., 2020), with 6 best features (dates)

(b) Proposed CIRE temporal features model

Figure 8. SHAP summary plots for the final models

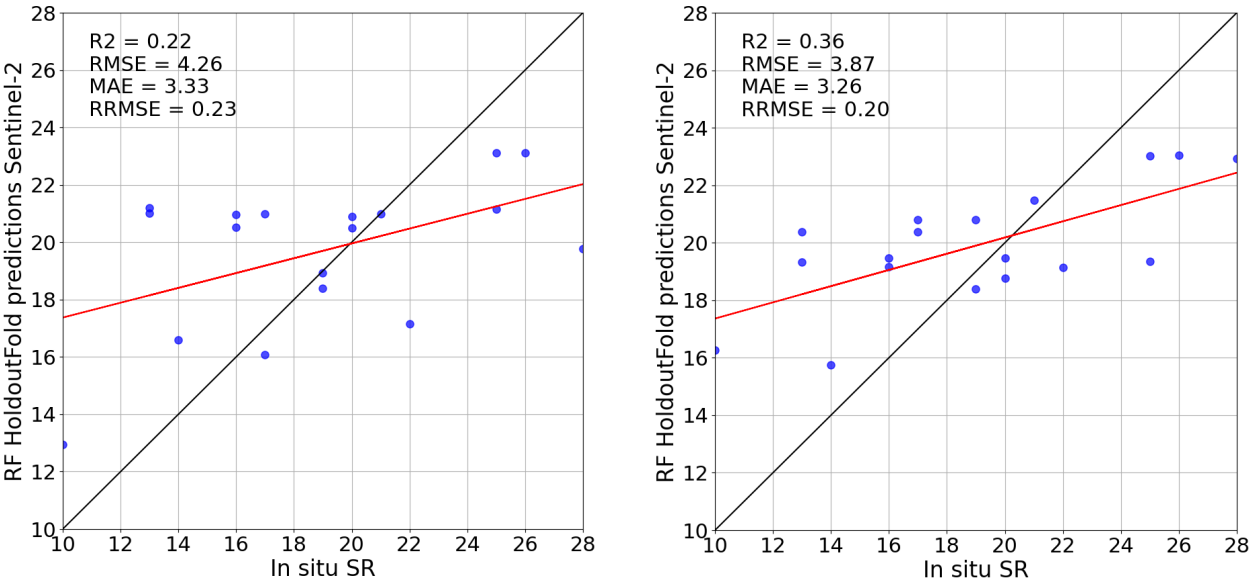

(a) RGB-NIR ts(6) baseline model (Fauvel et al., 2020), with 6 best features (dates)

(b) Proposed CIRE temporal features model

Figure 9. Holdout Species Richness (SR) predictions for the final models

This contribution has been peer-reviewed. The double-blind peer-review was conducted on the basis of the full paper.
https://doi.org/10.5194/isprs-annals-XI-3-2026-749-2026 | © Author(s) 2026. CC BY 4.0 License.

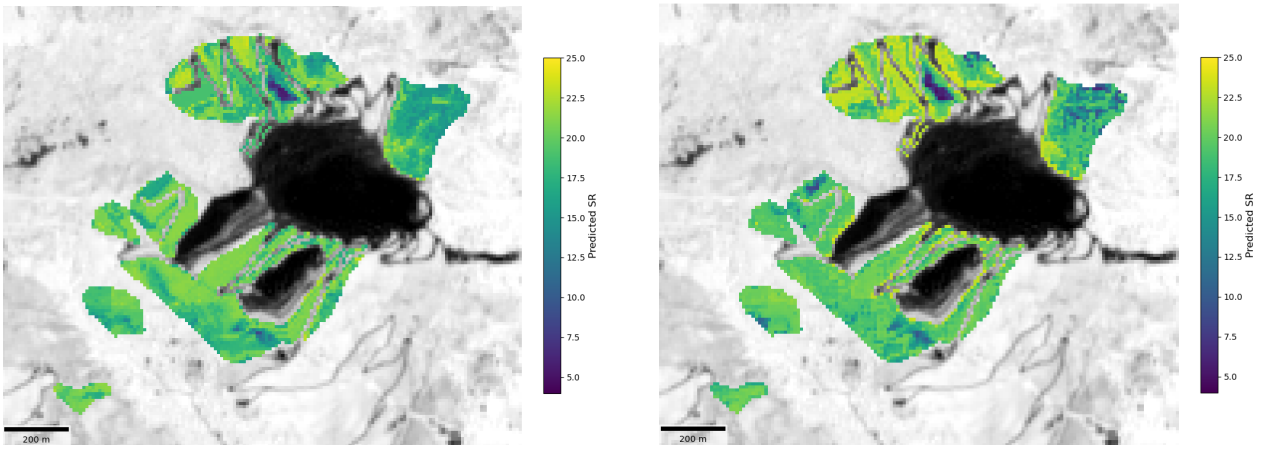

(a) RGB-NIR ts(6) baseline model (Fauvel et al., 2020), with 6 best features (dates)

(b) Proposed CIRE temporal features model

Figure 10. Wall-to-Wall Species Richness (SR) maps for the final models

series following (Muro et al., 2022) appeared prone to overfitting. The large set of band and date options introduced more noise than added value to the model pipeline. This highlights the need to summarize the temporal information by less features, as demonstrated by the impact of temporal fitting on model performance. To further reduce the reliance on RF feature selection, it would be beneficial to pre-filter which temporal features are inserted into the model pipeline with educated guesses. Additional experiments are being carried out on larger datasets available at other grassland sites, and will be published in the near future to strengthen results obtained in Hochfilzen.

For a small reference sample, individual observations can create noticeable shifts in the accuracy metrics. This partially explains why the prediction accuracy differed for the holdout versus the cross-validation dataset with regards to the CIRE temporal features. Despite ensuring similar distribution of diversity values and selecting quadrats all around the study area for both datasets, differences for example in the number of quadrat clusters remained. A majority of the five quadrat clusters were assigned to the cross-validation dataset and only one to the holdout.

The absolute performance of our best model was moderate for species richness estimation ($R^2 < 0.4$). However, it clearly outperformed baseline Sentinel-2 models on Hochfilzen data, illustrating the importance of summarizing temporal information into well crafted temporal features. Besides small sample size, this moderate performance could be partly explained by specific challenges at Hochfilzen site such as terrain or distribution of species richness. Performance would likely improve with integration of high resolution hyperspectral imagery, which is currently under investigation.

Although interesting patterns especially related to low diversity were found and confirmed by most of the compared models, quadrats with moderate diversity were challenging to discern from each other. The limited availability of high-diversity samples led regression models to under-estimate maximum diversity, especially if confounding factors, such as vegetation cover, caused any disagreement regarding the drivers of high diversity. Additionally, restricting the model complexity may have smoothed differences between quadrats. Further evaluation of the developed methodology at other sites with less complex revegetation patterns or a wider reference dataset may be necessary to confirm whether the unexplained portion of the diversity variation is related to the saturation of the found relationships or to the limited availability of reference data.

As the reference samples showed, species richness at revegetated sites can vary greatly within the 10m distance corresponding to the Sentinel-2 pixel footprint. Therefore, it was expected that the baseline models prioritized the higher resolution bands. As suggested by the holdout model comparison between the CIRE temporal features model and the corresponding 2-band (Red-Edge and NIR) model, temporal fitting may still find relevant patterns overlooked by the discrete temporal observations for coarser Red-Edge-based vegetation indices. The main challenge for the CIRE temporal features was accounting for the high variation in plant cover. One way to alleviate this could be to incorporate vegetation structure-related features, such as Fractional Vegetation Cover (FVC) or Leaf Area Index (LAI), into the model. The presence of occasional young trees may have also confounded the models, although we aimed to mitigate their impact by avoiding trees when defining the potential sampling locations.

In an alpine environment, several confounding factors related to snow cover duration, clouds, lighting conditions, and terrain features required mitigating actions. Some temporal features, such as the seasonal integral, seemed to benefit from normalization against the length of the growing season. Besides the growing season length, uneven snow cover duration impacted the extraction of phenological stages. It promoted extracting the peak season from a fitted time series rather than from a single date where phenological stages may be out of sync over the study area. The cloud cover challenges were mainly related to time series density. Fortunately for Hochfilzen, the lack of observed trends in the multiyear time series enabled aggregating succeeding years to increase the density of the Sentinel-2 time series. This decreased the dependency on image availability concerning certain seasonal key dates and allowed more robust detection of phenological events. In the next phase of this study, we plan to incorporate terrain features, such as slope direction, to account for the possible remaining confounding factors.

6. Conclusions

The proposed temporal fitting approach applied on relevant vegetation indices offers a promising way to capture plant species diversity related temporal patterns in Sentinel-2 time series

without inserting all observation dates. The proposed model trained on the best CIRE temporal features clearly outperformed all baseline models on the cross-validated and holdout sets across all accuracy metrics. When restricting baseline models to 6 features (dates), our best model still performed similarly on the cross-validation set, and better on the holdout set. This result highlights the importance of summarizing input time series data into time series descriptors, to improve species richness estimation in grasslands on a small study site.

However, for the Hochfilzen site characterized by complex revegetation patterns and limited reference data, only a small portion of the plant diversity variation was explained by any of the Sentinel-2 models, including baseline models. Nevertheless, we observed positive signals related to the importance of extracting temporal patterns from chlorophyll content related CIRE time series. Many of the most important features, such as amplitude, power at peak frequency and productivity, described the CIRE variation around the peak growing season. The risk of overfitting to local patterns and the sensitivity to total plant cover variation were found challenging.

Future studies should consider incorporating auxiliary data related to terrain features, plant cover and vegetation structure. To achieve a conclusive evaluation of the true potential of temporal fitting in species richness prediction from Sentinel-2 time series, the workflow should be implemented on a larger reference sample and more sites. A comparison of the proposed “temporal variation hypothesis” to the state of the art “spectral variation hypothesis” will also be performed, using full spectrum VNIR-SWIR hyperspectral imagery from drone and EnMAP images acquired in 2024.

The effectiveness of our methods will be evaluated in different biomes, types of grasslands, and stages of revegetation status. The proposed methodology is currently being applied in Sokli site, an early mining project in Northern Finland, and will be developed onto an operational service for Plant Diversity Estimation on top of GoldenRAM EO valued-adding platform.

7. Acknowledgements

This research is part of projects MultiMiner and GoldenRAM, funded by the European Union’s Horizon Europe research and innovations actions programme under Grant Agreement No. 101091374 and 101138153, respectively.

References

Cleveland, W. S., Devlin, S. J., 1988. Locally Weighted Regression: An Approach to Regression Analysis by Local Fitting. *Journal of the American Statistical Association*, 83(403), 596–610.

Fauvel, M., Lopes, M., Dubo, T., Rivers-Moore, J., Frison, P.-L., Gross, N., Ouin, A., 2020. Prediction of Plant Diversity in Grasslands Using Sentinel-1 and -2 Satellite Image Time Series. *Remote Sensing of Environment*, 237, 111536.

Lomb, N., 1976. Least-squares frequency analysis of unequally spaced data. *Astrophysics and Space Science*, 39, 447-462.

Lundberg, S. M., Lee, S.-I., 2017. A unified approach to interpreting model predictions. *Proceedings of the 31st International Conference on Neural Information Processing Systems (NIPS 2017)*, NIPS’17, Curran Associates Inc., Red Hook, NY, USA, 4768–4777.

McKenna, P. B., Lechner, A. M., Phinn, S., Erskine, P. D., 2020. Remote Sensing of Mine Site Rehabilitation for Ecological Outcomes: A Global Systematic Review. *Remote Sensing*, 12(21).

Molinier, M., Miettinen, J., Ienco, D., Qiu, S., zhu, Z., 2021. *Optical Satellite Image Time Series Analysis for Environment Applications: From Classical Methods to Deep Learning and Beyond*. John Wiley & Sons, Ltd, chapter 4, 109–154.

Muro, J., Linstädter, A., Magdon, P., Wöllauer, S., Männer, F. A., Schwarz, L.-M., Ghazaryan, G., Schultz, J., Malenovský, Z., Dubovyk, O., 2022. Predicting Plant Biomass and Species Richness in Temperate Grasslands across Regions, Time, and Land Management with Remote Sensing and Deep Learning. *Remote Sensing of Environment*, 282, 113262.

Ramsay, J., 2005. Functional Data Analysis. *Encyclopedia of Statistics in Behavioral Science*, John Wiley & Sons, Ltd.

Scargle, J. D., 1982. Studies in astronomical time series analysis. II - Statistical aspects of spectral analysis of unevenly spaced data. *The Astrophysical Journal*, 263, 835-853.

Yang, X., Lei, S., Xu, J., Zhao, Y., Tian, Y., Guo, Y., 2025. Mapping Alpha Diversity of Plant Species Using Scale Effects of Remote Sensing. *Ecological Informatics*, 86, 102993.

Zhou, Q., Zhu, Z., Xian, G., Li, C., 2022. A novel regression method for harmonic analysis of time series. *ISPRS Journal of Photogrammetry and Remote Sensing*, 185, 48-61.